Genomics Communications

ARTICLE

Open Access

https://doi.org/10.48130/gcomm-0025-0001

Genomics Communications **2025**, 2: e001

Characterization and comparative analysis of the first mitochondrial genome of *Michelia* (Magnoliaceae)

Suyan Wang[1,2#], Jing Qiu[3#], Ning Sun[2], Fuchuan Han[4], Zefu Wang[1], Yong Yang[1*] and Changwei Bi[1,2*]

[1] *State Key Laboratory of Tree Genetics and Breeding, Co-Innovation Center for Sustainable Forestry in Southern China, Key Laboratory of Tree Genetics and Biotechnology of Educational Department of China, Key Laboratory of Tree Genetics and Silvicultural Sciences of Jiangsu Province, Nanjing Forestry University, Nanjing 210037, China*

[2] *College of Information Science and Technology & Artificial Intelligence, Nanjing Forestry University, Nanjing 210037, China*

[3] *Information Department, The First Affiliated Hospital of Naval Medical University, Shanghai 200433, China*

[4] *Research Institute of Subtropical Forestry, Chinese Academy of Forestry, Fuyang 311400, China*

[#] Authors contributed equally: Suyan Wang, Jing Qiu

[*] Corresponding authors, E-mail: yangyong@njfu.edu.cn; bichwei@njfu.edu.cn

Abstract

Genus *Michelia* has various functions and is valuable in medicine, food, and agriculture. Many plastid genomes (plastomes) of *Michelia* have been released, but no mitochondrial genomes (mitogenomes) have been reported. In this study, using third-generation HIFI sequencing techniques, *Michelia figo* (*M. figo*) mitogenome was *de novo* assembled into a circular chromosome spanning 773,377 bp with a total GC content of 46.83%. Sixty six genes in total were annotated, including 41 protein-coding genes, 21 tRNA genes, and three rRNA genes. The mitogenome contains 1,514 dispersed repeats (> 30 bp), 39 tandem repeats, and 262 simple sequence repeats. Eighty one fragments originating from the *M. figo* plastome were detected in its mitogenome and three tRNA genes (*trnD-GUC*, *trnW-CCA*, and *trnV-GAC*) completely transferred from the plastome to the mitogenome. Repeats and collinearity analyses of four Magnoliaceae mitogenomes reveal substantial structural variations, a relatively low degree of collinearity, and significant genetic diversity of this genus. Phylogenetic analysis showed that two phylogenetic trees constructed separately based on mitogenomes and plastomes accurately depict the phylogenetic relationship of *M. figo*. This study offers the first comprehensive comparative genomic and phylogenetic analysis of the *M. figo* mitogenome, facilitating the development of genetic markers, taxonomic classification, and resource exploration within the *Michelia* genus.

Citation: Wang S, Qiu J, Sun N, Han F, Wang Z, et al. 2025. Characterization and comparative analysis of the first mitochondrial genome of *Michelia* (Magnoliaceae). *Genomics Communications* 2: e001 https://doi.org/10.48130/gcomm-0025-0001

Introduction

Mitochondria, as semi-autonomous organelles with their unique genetic material and systems, play crucial roles in plant energy metabolism by generating ATP through oxidative phosphorylation[1,2]. In plants, mitochondria not only participate in energy production, but also collaborate with other organelles to maintain cellular homeostasis[3]. In addition, mitochondria also participate in regulating processes such as apoptosis, playing an important regulatory role in plant life activities[4]. However, despite the undisputed significance of mitochondria, previous research on plant mitochondrial genomes (mitogenomes) has been scant. Initially, sequencing and assembly techniques which were primarily developed for nuclear genomes, encountered significant challenges in handling mitogenomes due to their complicated structures, leading to fragmented or incomplete mitogenome assemblies. Moreover, early bioinformatic tools were not optimized for the unique characteristics of mitogenomes. This limitation further hindered the accurate assembly and analysis of plant mitogenomes. Nevertheless, with the continuous advancement of sequencing technology, especially the widespread application of long-read sequencing, research on plant mitogenomes has gradually increased in recent years[5–8].

The mitogenomes of most higher plants exhibit substantial variability in structure and size[9]. Plant mitogenomes contain numerous repetitive sequences (repeats), leading to significant variations in size and structure through frequent recombination events[10]. The size of plant mitogenomes is 100–1,000 times larger than that of animals (15-18 kb)[11]. Plant mitogenomes stand out not just for their exceptional size, but also for the notable variation in size they display across diverse species. For example, *Viscum scurruloideum*[12] has a mitogenome of only 66 kb, while the mitogenome of *Larix sibirica* is 11.7 Mb[13]. Additionally, the intricate structure of plant mitogenomes further adds to their complexity, with most of them existing as a single circular molecule, while a minority exist as linear or branched molecules. It has been reported that the mitogenomes of *Populus simonii*[14] and *Fagopyrum esculentum*[15] are composed of three and ten circular molecules, respectively. Although plant mitogenomes differ significantly in terms of size and structure, the number of genes remains comparably stable and conserved, with a similar core set of PCGs, rRNAs, and tRNAs which are essential for respiratory function, and translation processes[16]. Intracellular gene transfer (IGT) can further complicate the mitogenome, as sequences from both the plastid and nuclear genomes coexist in plant mitogenomes[17]. For instance, the sequences of the nuclear and plastid genomes account for 46.5% and 1.4% of the *Cucumis melo* mitogenome, respectively[18]. Therefore, the plant mitogenome, due to its complex characteristics, is an ideal system for exploring genome complexity.

Michelia figo (*M. figo*) belongs to the genus *Michelia* of the Magnoliaceae family, which is the second-largest genus and a relatively evolved group in the Magnoliaceae family. There are about 80 *Michelia* species in the world, predominantly distributed in tropical, subtropical, and temperate regions of Asia, of which approximately 70 species are distributed in China[19,20]. The broad spectrum of physiological activities exhibited by the genus *Michelia* underscores its potential applications in medicine, food, agriculture, and other domains[21]. The flowers, leaves, branches, and other parts of these species contain abundant aromatic oil that has been traditionally

used in China, India, and other regions for treating fever, leprosy, inflammation, and other ailments[22]. *Michelia* species usually serve as valuable sources of bioactive compounds, exhibiting antibacterial[23], and antioxidant properties[24]. Furthermore, the methanolic extract from the leaves of *M. figo* has a concentration-dependent vasodilatory effect, having widespread applications in medicine[25].

A previous study has reported the complete plastome of *M. figo* and analyzed its phylogenetic relationship with other *Michelia* species based on (plastid genomes) plastomes[26]. However, the mitogenome of *M. figo* and its phylogenetic status based on mitogenomes remain unexplored. Additionally, many plastomes of *Michelia* have been released[27–29], but no mitogenomes have been reported for this genus. Consequently, to further explore the evolution and genetics of *M. figo*, this study has successfully assembled the complete mitogenome of *M. figo*. Comparative genomic and phylogenetic analyses were undertaken to elucidate the characteristics of the mitogenomes of *M. figo* and other Magnoliaceae species. These analyses will offer crucial theoretical and data-driven supports for genomic research, biological functions, and mitogenome evolution in *M. figo* and other *Michelia* species.

Materials and methods

DNA extraction and sequencing

In this study, we collected fresh leaves of *M. figo* at Nanjing Forestry University, Nanjing, Jiangsu Province, China (118.81° E, 32.07° S). Before DNA extraction, fresh leaves were immediately frozen in liquid nitrogen to preserve their integrity and subsequently stored in a laboratory freezer maintained at −80 °C. The total genomic DNA was extracted using the CTAB method[30]. The quality of the DNA sample was evaluated using 1% agarose gel electrophoresis, while its concentration was accurately determined using a NanoDrop ND 2000 (ThermoFisher Scientific, Waltham, MA, USA)[31]. The size of the genomic insert fragments is 15–18 kb. Then the sequencing libraries were constructed using the high-integrity genomic DNA through SMRTbell Express Template Prep Kit 2.0 (PacBio Biosciences, Menlo Park, CA, USA). We ultimately obtained the HiFi sequencing data from the PacBio Revio platform.

Mitogenome assembly and annotation

The HiFi sequencing data was fed into PMAT v1.31[32] to assemble the mitogenome of *M. figo*. The parameters were 'autoMito -st hifi -g 2.2G -CPU 50'. The nuclear genome size of *M. figo* was estimated using the genome of *Magnolia biondii* as a reference[33]. After using PMAT, the raw assembly graph of *M. figo* mitogenome was composed of 12 contigs, containing four pairs of repeats. Using Bandage[34], we obtained the circular mitogenome of *M. figo* by decoding the raw assembly graph, taking into account the copy number of each contig. The mitogenome of *M. figo* was annotated using the online program PMGA[35]. The rRNA and tRNA genes were then verified by BLASTN[36] and tRNAscan-SE v2.0[37], respectively. Finally, an online tool PMGmap[38] was used to draw the mitogenome map.

Analysis of repeats and codon usage

The online tool MISA[39] was used to detect simple sequence repeats (SSRs) of the *M. figo*, *M. biondii*, and *M. officinalis* mitogenomes. We set the repetition thresholds at 10, 5, 4, 3, 3, and 3 for mononucleotides, dinucleotides, trinucleotides, tetranucleotides, pentanucleotides, and hexanucleotides, respectively. The minimal distance between two SSRs was established as 100 bp. Meanwhile, the online tool TRF[40] was utilized to detect tandem repeats with default parameters. REPuter[41] was used to detect dispersed repeats and the parameters were set as follows: hamming distance of three, maximum computed repeats of 5000, and a minimal repeat size of 30 bp[42]. Codon composition and usage of the *M. figo* mitogenome were analyzed using CondonW v1.4.4 (https://codonw.sourceforge.net/) with default parameters.

Mitochondrial plastid transfer (MTPT) and collinearity analysis

We obtained the plastid genome (plastome) of *M. figo* from the NCBI with the accession number of NC_053861.1. Then, we used BLASTN[36] to identify the homologous fragments between the mitogenome and plastome, and utilized TBtools to visualize the results[43]. We selected three mitogenomes of Magnoliaceae (*L. tulipifera*, *M. biondii,* and *M. officinalis*) for the collinearity analysis with *M. figo*. The collinear blocks were identified using MUMmer v4.0[44] with default parameters. We chose collinear blocks that exceeded 5,000 bp for subsequent analysis. NGenomeSyn v1.0[45] was finally used to visualize the results.

Phylogenetic analysis

To further clarify the phylogenetic location of *M. figo*, two phylogenetic trees were constructed using 15 plant mitogenomes and plastomes respectively, including two species of Gymnosperm (*Cycas taitungensis*, and *Ginkgo biloba*), three species of ANA clade (*Amborella trichopoda*, *Nymphaea colorata*, and *Schisandra sphenanthera*), four species of Magnoliidae (*L. tulipifera*, *M. figo*, *M. officinalis*, and *M. biondii*), three species of monocots (*Apostasia shenzhenica*, *Cocos nucifera*, and *Sorghum bicolor*), and three species of core eudicots (*Ilex pubescens*, *Sapindis mukorossi*, and *Ficus carica*). Among these plant species, *C. taitungensis* and *G. biloba* were selected as outgroups. We used in-house Python scripts to select shared genes and used MAFFT v7.407[46] to compare the shared genes. After trimming the results using trimAl v1.4[47], IQ-TREE v2.0.3[48] was utilized to construct the phylogenetic trees based on the maximum likelihood (ML) method with 1,000 bootstraps.[49]. Both plastid and mitochondrial trees were found to be best fit by the GTR + F + I + G4 model. Finally, the online tool iTOL[50] was used to visualize and optimize the results.

Results

Mitogenome features of *M. figo*

Using the Revio sequencing platform, we obtained a total of 410,107 HiFi sequencing reads with 5.83 Gb in length and the N50 value of 14,355 bp. After using PMAT v1.31 to generate the raw assembly graph of the *M. figo* mitogenome (Fig. 1a), we utilized Bandage to disentangle the mitogenome graph resulting in a circular molecule with 773,377 bp in length (Fig. 1b). The total GC content is 46.83%, with 26.56%, 26.21%, 23.37%, and 23.46% for bases A, T, G, and C, respectively. The *M. figo* mitogenome was annotated with 66 genes, comprising 41 protein-coding genes (PCGs), 21tRNA, and three rRNA, as detailed in Table 1. Figure 1c provides a visual representation of the functional classification and specific positions of the annotated genes. The majority of genes are present in a single-copy format, with the exception of three genes (*rps7*, *trnM-CAU*, and *trnP-UGG*), possessing multiple copies. Moreover, we found that a total of 10 genes harbor introns (*ccmFc*, *rpl2*, *rps3*, *rps10*, *cox2*, *nad1*, *nad2*, *nad4*, *nad5*, and *nad7*) (Supplementary Fig. S1). Most of these introns are *cis*-spliced, with *nad1*, *nad2,* and *nad5* containing a few *trans*-spliced introns.

Analysis of codon usage

The relative synonymous codon usage (RSCU) value is equal to 1 when there is no synonymous codon usage preference. In the *M. figo* mitogenome, the RSCU values of AUG (Met), UGG (Trp), and AGC (Ser) are 1 (Supplementary Table S1). Twenty nine codons exhibit RSCU values above 1, among which the codon AGA (Arg) possesses the highest RSCU value, especially 1.57. Additionally, the RSCU values of 32 codons are lower than 1, with CGU(Arg) exhibiting the lowest RSCU value of 0.64. We also compared the RSCU of *M. figo* mitogenome with

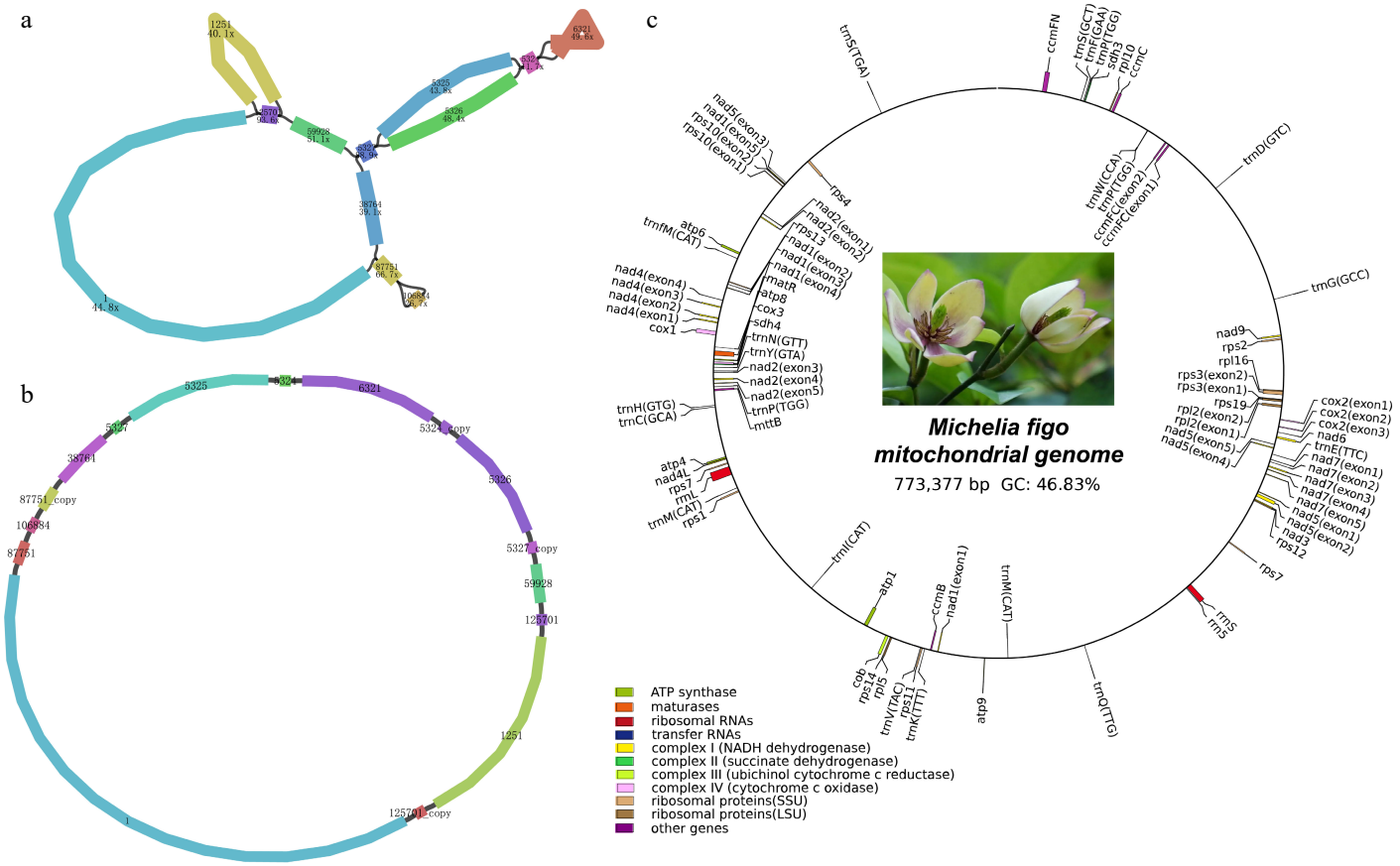

Fig. 1 Structural and functional features of the *M. figo* mitogenome. (a) The raw assembly graph of the *M. figo* mitogenome. (b) The disentangled graph of the *M. figo* mitogenome. (c) Circular mitogenome map of *M. figo*. Genes depicted outside the outer circle undergo clockwise transcription, while those positioned within the inner circle undergo counter-clockwise transcription. The legends of different colors positioned in the bottom left corner serve to distinguish genes based on their specific functionalities.

the other three Magnoliaceae mitogenomes. The result shows that the relative synonymous codon usage is highly consistent (Fig. 2a), with the codon of AGA (Arg) exhibiting the highest RSCU value in these mitogenomes (Supplementary Table S1). We further calculated the frequency of codon usage, revealing a remarkable similarity across the mitogenomes of Magnoliaceae (Fig. 2b & Supplementary Table S2).

Analysis of repeats

The *M. figo* mitogenome contains abundant repeats (Fig. 3). Using the online tool REPuter, we detected 1,514 pairs of dispersed repeats (≥ 30 bp), including 758 pairs of forward repeats and 756 pairs of palindromic repeats (Supplementary Table S3). However, there are no complementary and reverse repeats. Additionally, the *M. figo* mitogenome was found to harbor 39 tandem repeats, with lengths varying from 14 to 52 bp (Supplementary Table S4), with matching identity greater than 64%. Altogether, 262 SSRs were identified in the *M. figo* mitogenome (Supplementary Table S5), most of which are tetranucleotides (96), followed by mononucleotides (55), and dinucleotides (55).

To further investigate the repeats in the mitogenomes of Magnoliaceae, we detected and compared the tandem, SSRs and dispersed repeats in the mitogenomes of three Magnoliaceae species (*M. biondii*, *M. officinalis*, and *M. figo*). The results show that only *M. officinalis* contains two pairs of reverse repeats and one pair of complementary repeats (Fig. 4a), while the number of tandem repeats does not exhibit significant variation (Supplementary Tables S6 & S7). The *M. officinalis* mitogenome exhibits the highest number of dispersed repeats (3,609), followed by *M. biondii* (2,800) and *M. figo* (1,514) (Fig. 4a, Supplementary Tables S8 & S9). The distribution of dispersed repeat lengths across the three mitogenomes is also similar (Fig. 4b), with most repeats ranging from 30 to 49 bp, and only a few exceeding 500 bp. Additionally, comparative results of SSRs reveal that all three mitogenomes of Magnoliaceae contain six SSR types (Fig. 4c, Supplementary Tables S10 & S11), with *M. officinalis* exhibiting the highest number of SSRs (327). The diversity of SSR types in Magnoliaceae mitogenomes does not vary significantly, with the exception of a notable difference in the case of mononucleotides.

Analysis of MTPTs

We identified 81 fragments transferred from the plastome to the mitogenome of *M. figo* (Fig. 5 & Supplementary Table S12), ranging from 50 to 4,665 bp. The entire length of MTPTs measures 42,791 bp, constituting 5.53% of the whole mitogenome. Most of these MTPTs range from 50 to 500 bp in length, and only 11 fragments exceeding 1 kb, with the longest fragment reaching 4,666 bp. A total of 15 plastid genes were found to be located on MTPTs, including nine PCGs (*psbL*, *psbF*, *psbE*, *petL*, *petG*, *rps8*, *rpl14*, *rps7*, and *ndhB*) and six tRNA genes (*trnD-GUC*, *trnY-GUA*, *trnE-UUC*, *trnW-CCA*, *trnP-UGG*, and *trnV-GAC*). Notably, *trnD-GUC*, *trnW-CCA*, and *trnV-GAC* are completely transferred from the plastome to the mitogenome. Additionally, we found that MTPT22, MTPT65, MTPT68, and MTPT69 are located in repeat regions.

Collinearity analysis of four Magnoliaceae mitogenomes

We conducted a collinearity analysis by comparing the mitogenome of *M. figo* with three other Magnoliaceae mitogenomes (*L. tulipifera*,

Table 1. Gene compositions of the *Michelia figo* mitogenome.

Group of genes	Name	Start codon	Stop codon	Length	Amino acids
ATP synthase	*atp1*	ATG	TGA	1,530	509
	atp4	ATG	TAA	582	193
	atp6	ATG	TAG	891	296
	atp8	ATG	TAA	480	159
	atp9	ATG	TAA	261	86
Cytochrome c biogenesis	*ccmB*	ATG	TGA	621	206
	ccmC	ATG	TAA	960	319
	*ccmFc**	ATG	TAA	1,359	452
	ccmFn	ATG	TAG	1,806	602
Ubichinol cytochrome c reductase	*cob*	ATG	TGA	1,182	393
Cytochrome c oxidase	*cox1*	ACG	TAA	1,584	527
	*cox2***	ATG	TAA	759	252
	cox3	ATG	TGA	798	265
Maturases	*matR*	ATG	TAG	1,959	652
Transport membrane protein	*mttB*	ACG	TGA	768	255
NADH dehydrogenase	*nad1****+	ACG	TAA	978	325
	*nad2*****	ATG	TAA	1,467	488
	nad3	ATG	TAA	357	118
	*nad4****	ATG	TGA	1,488	495
	nad4L	ACG	TAA	303	100
	*nad5***++	ATG	TAA	2,013	670
	nad6	ATG	TGA	735	244
	*nad7*****	ATG	TAG	1,185	394
	nad9	ATG	TAA	573	190
Large subunit of ribosome (LSU)	*rpl10*	ATG	TAA	471	156
	rpl16	GTG	TAA	435	144
	*rpl2**	ATG	TAG	1,665	697
	rpl5	ATG	TAA	561	186
Small subunit of ribosome (SSU)	*rps1*	ATG	TAA	606	201
	*rps10**	ATG	TGA	420	139
	rps11	ATG	TGA	552	183
	rps12	ATG	TGA	378	125
	rps13	ATG	TGA	351	116
	rps14	ATG	TAG	303	100
	rps19	ATG	TAA	282	93
	rps2	ATG	TAA	657	218
	*rps3**	ATG	TAA	1,572	523
	rps4	ACG	TAA	1,071	356
	rps7 (2)	ATG/ATG	TAA/TAA	450	149
Succinate dehydrogenase	*sdh3*	ATG	TAA	330	109
	sdh4	ATG	TGA	447	148
Ribosomal RNAs	*rrn5*	–	–	117	–
	rrnL	–	–	3,560	–
	rrnS	–	–	2,087	–
Transfer RNAs	*trnC-GCA*	–	–	71	–
	trnD-GUC	–	–	74	–
	trnE-UUC	–	–	72	–
	trnF-GAA	–	–	74	–
	trnfM-CAU	–	–	74	–
	trnG-GCC	–	–	73	–
	trnH-GUG	–	–	74	–
	trnI-CAU	–	–	81	–
	trnK-UUU	–	–	73	–
	trnM-CAU (2)	–	–	73/73	–
	trnN-GUU	–	–	72	–
	trnP-UGG (3)	–	–	75/74/75	–
	trnQ-UUG	–	–	72	–
	trnS-GCU	–	–	88	–
	trnS-UGA	–	–	87	–
	trnV-UAC	–	–	73	–
	trnW-CCA	–	–	74	–
	trnY-GUA	–	–	83	–

* Indicates the *cis*-spliced introns, and + indicates the *trans*-spliced introns. The number of * and + represents the number of introns. The number in parentheses represents the number of genes.

M. officinalis, and *M. biondii*). As illustrated in Fig. 6a, a total of 40 locally collinear blocks (LCBs) were identified between the mitogenomes of *M. figo* and *M. officinalis* (Supplementary Table S13). The cumulative length of these colinear blocks amounts to 416,577 bp, comprising approximately 53.86% of the *M. figo* mitogenome. Among these colinear blocks, the longest is 34,737 bp, and the average length is 10,413 bp. Between the mitogenomes of *M. biondii* and *M. figo*, we detected 42 LCBs, accounting for 59.04% (456,622 bp) of the *M. figo* mitogenome (Supplementary Table S14). The longest colinear block is 44,187 bp, and the average length is 10,871 bp. Between the mitogenomes of *M. biondii* and *L. tulipifera*, a total of 27 LCBs were identified (Supplementary Table S15), accounting for 52.14% (287,725 bp) of the *L. tulipifera* mitogenome. The longest colinear block is 30,420 bp, and the average length is 10,656 bp. The average colinear lengths of the four mitogenomes are highly consistent (Fig. 6b).

Phylogenetic analysis

To further elucidate the phylogenetic position of *M. figo*, we constructed two phylogenetic trees based on 18 mitochondrial and 61 plastid PCGs from 15 species, respectively (Supplementary Tables S16 & S17). As illustrated in Fig. 7, 91.67% of the total nodes possess bootstrap support values exceeding 80%, including 20 nodes that achieve the maximum support of 100%. From the basal group downward, the bootstrap value for the separation of Magnoliidae from the clade consisting of monocots and core eudicots is 100%. In the Magnoliidae, the bootstrap value for the separation of Magnoliales and Laurales is 100%. Furthermore, we found that *M. biondii* and *M. officinalis* firstly grouped, this clade subsequently grouped with *M. figo* with a 100% bootstrap value, indicating that *Michelia* is closely related to *Magnolia*. The phylogenetic trees constructed based on mitogenomes and plastomes exhibit remarkable consistency, supporting that *Michelia* is closely related to *Magnolia*.

Discussion

Plant mitogenomes frequently undergo recombination events mediated by repeats, resulting in great differences in their size[51]. Despite the closely related species, notable variations in mitogenome size can still be observed. For example, the size of the *Silene latifolia* mitogenome (253 kb) differs by 45 times compared to that of *S. conica* (11.3 Mb)[52]. The mitogenomes of *Cucumis melo* (2.9 Mb) and *Citrullus lanatus* (379 kb) differ by more than seven times[53]. The frequent recombination events of plant mitogenomes may integrate a large amount of foreign DNA during evolution, potentially contributing to the great differences in plant mitogenomes size. In this study, the mitogenome length of *M. figo* (773,377 bp) is relatively short in Magnoliaceae, with the longest in *M. biondii* (967,100 bp), followed by *M. officinalis* (930,306 bp) and *M. liliiflora* (865,191 bp). The shortest mitogenome is *L. tulipifera* (551,806 bp), accounting for only 60% of the mitogenomes of *M. biondii* and *M. officinalis*.

Frequent recombination events not only lead to great differences in mitogenome size, but also contribute to complex and diverse structures of plant mitogenomes[54], ranging from single circular and linear structures to more complex branched linear, branched circular, and other complex structures[55]. It has been reported that the mitogenomes of *Amborella trichopoda*[56], *Rhopalocnemis phalloi*[57], and *Panax notoginseng*[58] are complex dynamic structures resulting from recombination. The mitogenome structures of Magnoliaceae are relatively conserved, with the majority being assembled into a single circular chromosome (*M. biondii*, *M. officinalis*, *M. figo*, and *L. tulipifera*). However, the mitogenome of *M. liliiflora* exhibits a linear chromosome. Additionally, the mitogenomes of angiosperms exhibit rapid structural differentiation and loss of collinearity, even

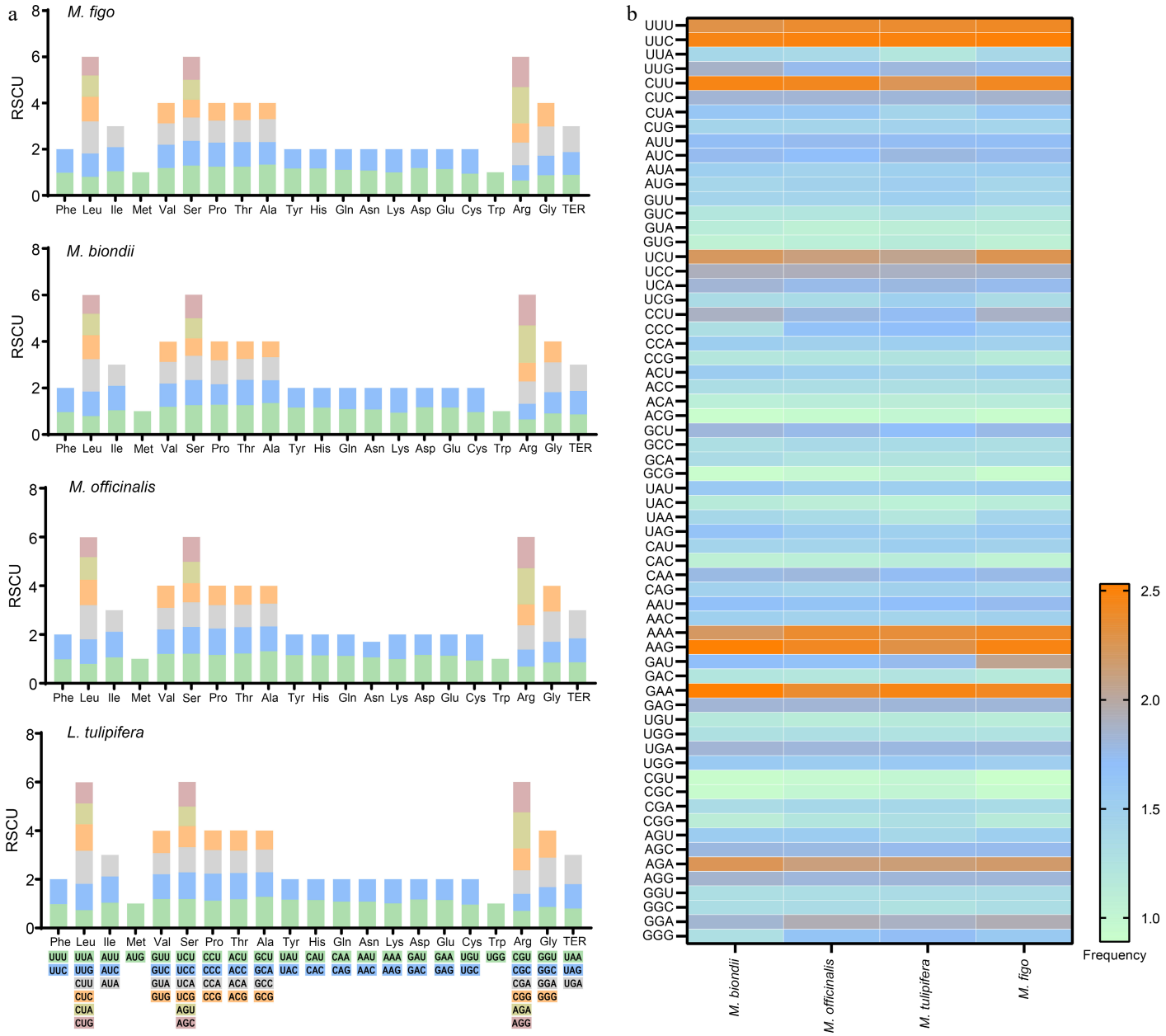

Fig. 2 Codon usage of four Magnoliaceae mitogenomes. (a) Stacked column plots of the relative synonymous codon usage. (b) Heatmap of the codon usage frequencies.

those of closely related species[59,60]. In this study, using the nucmer program of MUMmer, numerous colinear regions and genomic rearrangements were identified among four Magnoliaceae mitogenomes. The lengths of these colinear blocks account for more than half of each mitogenome. The results of collinearity analysis reveal there may have been significant genomic rearrangements in the mitogenomes of Magnoliaceae species during their evolutionary history.

The mitogenomes of angiosperms generally encode a core set of 24 PCGs: *nad1-7*, *9*, and *4L*; *cob*; *cox1-3*; *ccmB*, *C*, *Fc*, and *Fn*; *atp1*, *4*, *6*, *8*, and *9*; *mttB*/*tatC*; and *matR*. Although these core genes are present in most mitogenomes, there are significant variations in their quantity, position, and arrangement, even within mutants of the same species. In addition to the 24 conserved PCGs, plant mitogenomes also possess 19 standard variable genes, consisting of five large subunits of ribosome proteins (*rpl2*, *5*, *6*, *10*, and *16*), 12 small subunits of ribosome proteins (*rps1-4*, *7*, *8*, *10-14*, and *19*), and two respiratory genes (*sdh3-4*). Among these variable genes, the large and small subunits of ribosome genes are missing relatively frequently[61]. The mitogenome of *M. figo* harbors all 24 core PCGs, with only two variable PCGs (*rpl6* and *rps18*) being lost. Similarly, the mitogenomes of *M. biondii*[33] and *L. tulipifera*[62] have retained nearly all ancestral PCGs. However, the *Silene vulgaris* mitogenome has nearly lost all variable PCGs with the exception of *rps13*. Moreover, the *Viscum scurruloideum* mitogenome has lost the entirety of 11 of the 24 core PCGs, including *ccmB*, *matR*, and all NADH dehydrogenase genes[12]. The gene content in the mitogenomes of Magnoliaceae is relatively abundant[63], suggesting that they may have undergone less gene loss during the mitogenome evolution.

Plant mitogenomes vary significantly in the number of introns. The *Silene latifolia* mitogenome has only 19 introns[64], while the *Selaginella moellendorffii* mitogenome contains the largest number of 37 introns[65]. The *M. figo* mitogenome contains 25 introns in 10 PCGs (*ccmFc*, *rpl2*, *rps3*, *rps10*, *cox2*, *nad1*, *nad2*, *nad4*, *nad5*, and

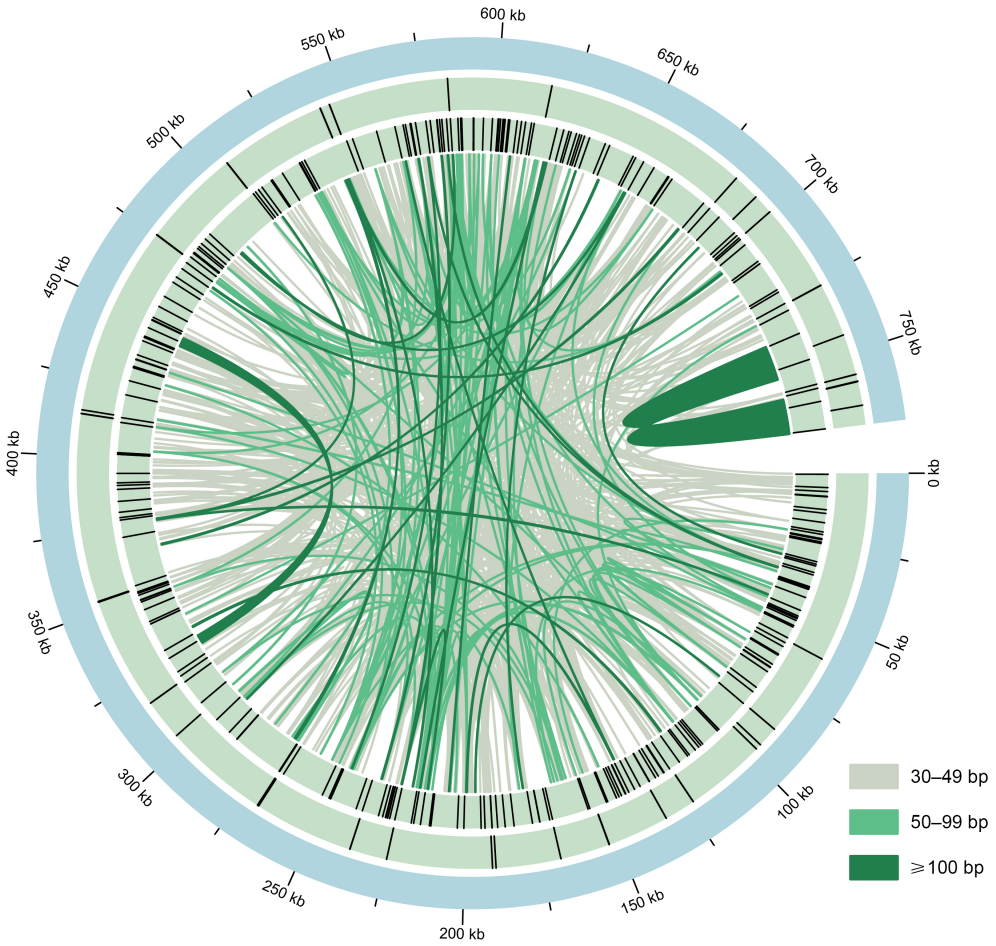

Fig. 3 The distribution of repeats in the *M. figo* mitogenome. From the center outward, the first circle shows the mitogenome of *M. figo*, the second and third circle shows tandem repeats and simple sequence repeats, respectively. The inner lines represent the dispersed repeats. The legends of different colors positioned in the bottom left corner represent the dispersed repeats of different lengths.

nad7), consisting of 22 *cis*-splicing and three *trans*-splicing introns. *Cis*-splicing is prevalent in most introns of angiosperm mitogenomes, whereas *nad1*, *nad2,* and *nad5* evolved a split structure that requires *trans*-splicing[63]. Similar to the majority of angiosperm mitogenomes, the intron rps3i257 in the *M. figo* mitogenome is completely lost during differentiation[66]. These results indicate that introns are frequently gained or lost during the evolution of plant mitogenomes (Supplementary Fig. S2)[63].

Plant mitogenomes are characterized by the abundance of repeats, contributing to the complexity and diversity of mitogenome sizes and structures through frequent recombination events[10]. The intense recombination events mediated by long repeats (> 500 bp) facilitate reversible recombination, regulate the molecular conformation of the mitogenome, and ultimately contribute to the expansion and complexity of plant mitogenomes[54]. In this study, the *M. figo* mitogenome exhibits the lowest abundance of SSRs and long repeats (> 500 bp), whereas *M. biondii* mitogenome displays the highest abundance in Magnoliaceae. It can be inferred that it is likely to undergo less recombination events during the evolution of *M. figo* mitogenome, while the *M. biondii* mitogenome may experience more recombination events. Simultaneously, variations in the quantity of repeats may result in significant differences in the size of mitogenomes. For example, the mitogenome sizes of bryophytes remain relatively stable at approximately 110 kb, probably due to the scarcity of repeats within their mitogenomes. This scarcity contributes to the conserved and stable structure of the bryophyte mitogenomes. By contrast, the mitogenomes of ferns exhibit a significant number of repeats, accounting for their relatively large sizes[10]. In this study, the mitogenomes of *M. biondii* and *M. officinalis* exhibit a significantly higher numbers of repeats compared to *M. figo*, potentially explaining the differences in their mitogenome sizes.

DNA fragment transfer events between the plastomes and mitogenome, as well as among different species, are recurrent phenomena that occur during the evolution of the plant mitogenome[67]. The lengths and similarities of these cp-derived fragments vary among different species[68]. The total length of MTPTs in the *M. figo* mitogenome is 42,791 bp, constituting 5.53% of the whole mitogenome. This proportion is significantly higher than that observed in numerous other mitogenomes, such as *Arabidopsis thaliana* (0.8%) , *Glycine max* (0.6%), *Silene conica* (0.2%), and *Vigna angularis* (0.1%)[69]. At the other extreme, the length of MTPTs accounts for 10.5% of the *Boea hygrometrica* mitogenome[70]. The MTPTs in the *M. figo* mitogenome are notably abundant, with the longest fragment spanning 4,666 bp, and the majority of MTPTs ranging from 50 to 500 bp. These sizable MTPTs are presumed to have significant impacts on plant mitogenome evolution, thereby contributing to genetic diversity[17,71]. Additionally, it is frequently observed that these transferred fragments contain PCGs. The number of PCGs in MTPTs exhibits significant variation in plant mitogenomes, ranging from seven in *Brassica* to 22 in *Nicotiana*[72]. In the mitogenome of *M. figo*, nine PCGs (*psbL*, *psbF*, *psbE*, *petL*, *petG*, *rps8*, *rpl14, rps7*, and *ndhB*) are located in MTPTs. However, PCGs in MTPTs turned out to degenerate as a result of sequence alterations and the absence of

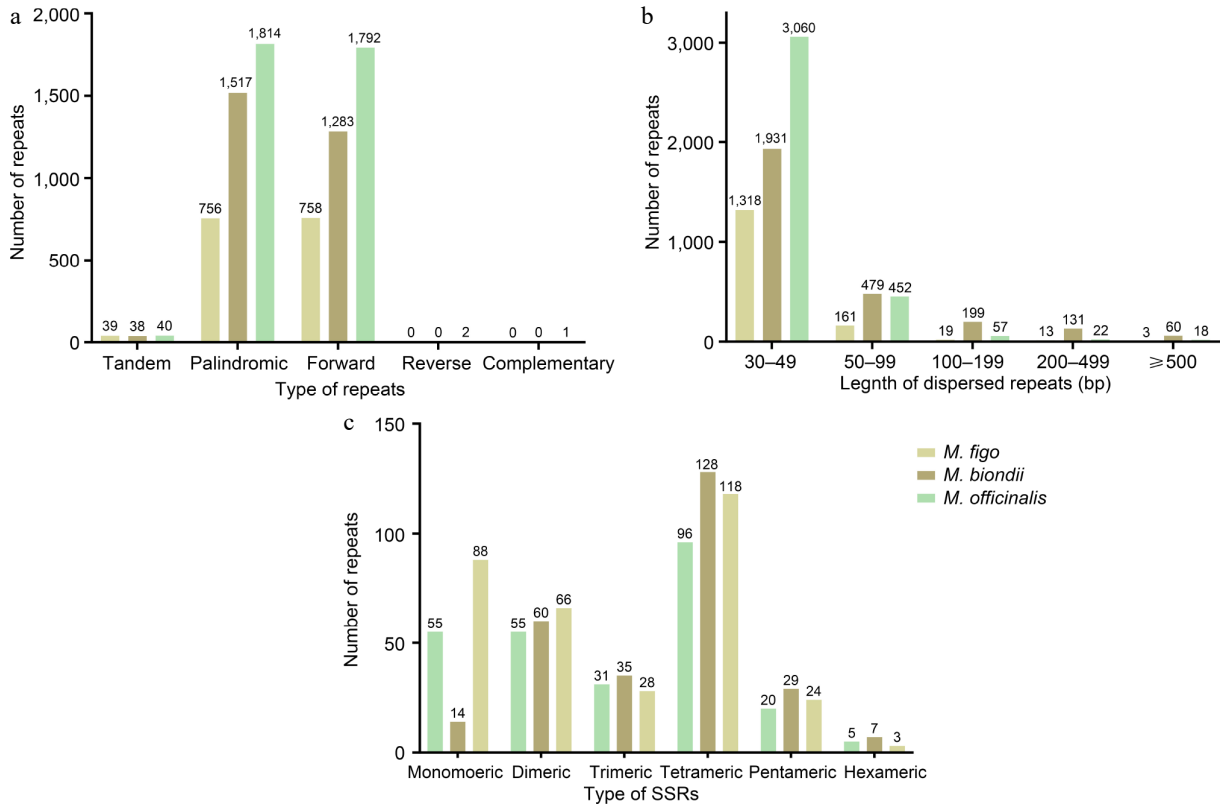

Fig. 4 (a) Type and number of simple sequence repeats in the mitogenomes of two Magnolia species and *M. figo*. (b) Length and number of dispersed repeats in the mitogenomes of two Magnolia species and *M. figo*. (c) The different colored legends indicate different species.

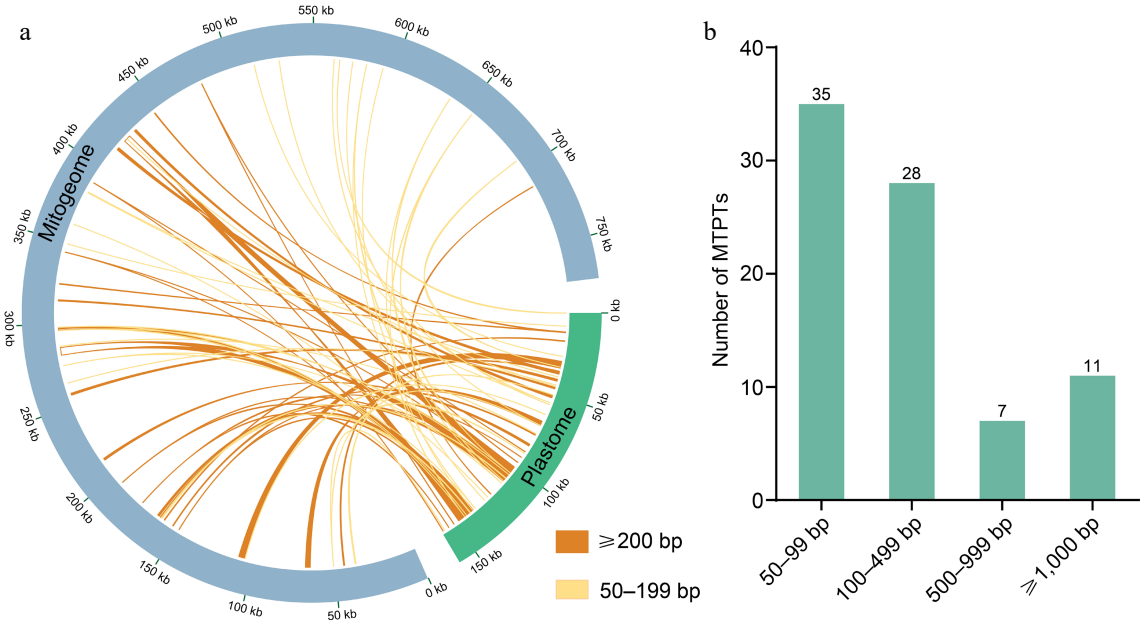

Fig. 5 (a) Homologous sequences between mitogenome and plastome. The plastome is represented by the green circular segment and the mitogenome by the gray circular segment, and two different kinds of yellow lines represent the homologous fragments. The legends of different colors positioned in the bottom right corner represent fragments of different lengths. (b) Lengths and numbers of these homologous fragments in the *M. figo* mitogenome.

RNA editing[73,74]. Consequently, PCGs in MTPTs may have limited functional significance in mitogenomes, potentially acting as non-essential sequences[72].

In this study, we reconstructed two phylogenetic trees based on 18 mitochondrial and 61 plastid PCGs from 15 species, respectively. Both trees exhibit remarkable consistency, supporting that *Michelia* is closely related to *Magnolia*, which is consistent with previous studies[26,75]. Additionally, the topological structure of the two phylogenetic trees is also highly consistent with the Angiosperm Phylogeny Group IV (APG IV) system[76]. However, due to the scarcity of mitogenomes in *Michelia*, we are unable to expand our discussion on the phylogenetic relationships in this genus.

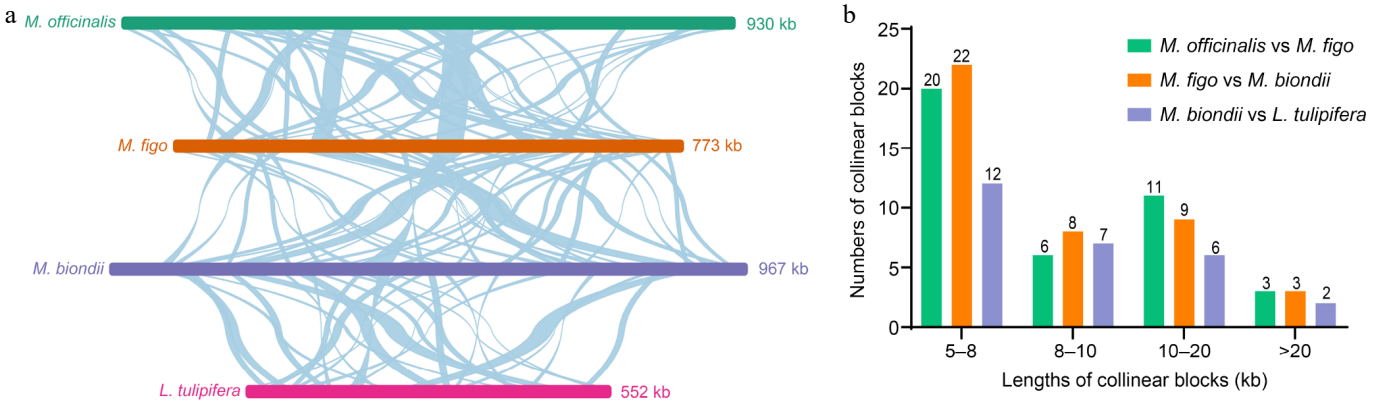

Fig. 6 Schematic representation of the collinearity among four Magnoliaceae mitogenomes. (a) Collinearity plots of the four Magnoliaceae mitogenomes. The mitogenomes are shown by the bars in each row, and collinear regions are indicated by the connecting lines in the center. (b) Lengths and numbers of collinear blocks. The different colored legends indicate homologous fragments between different species.

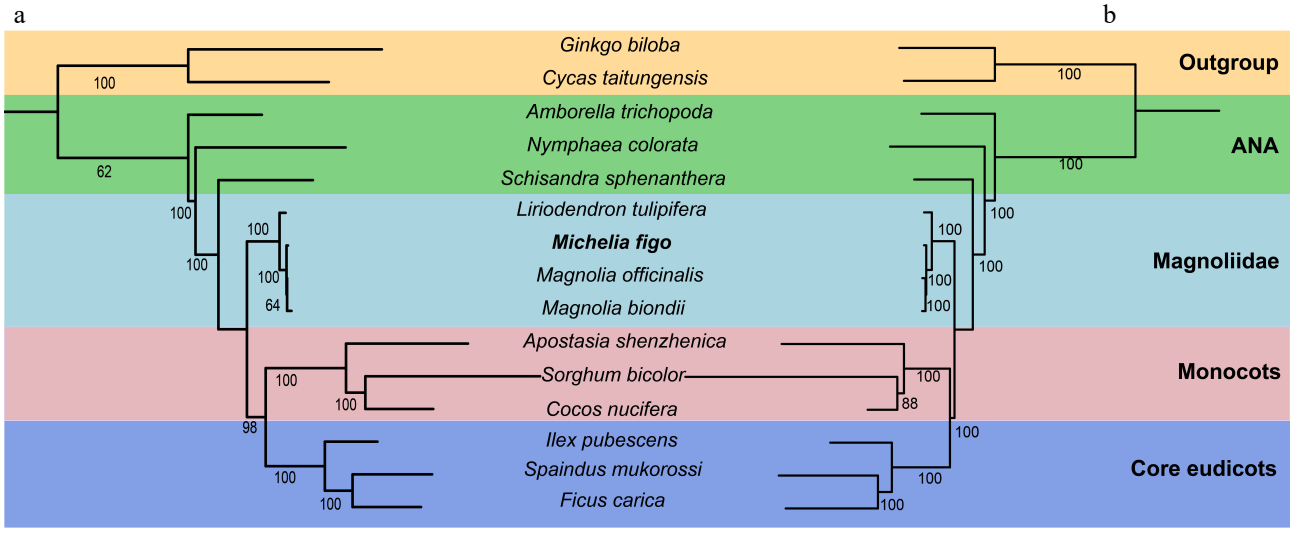

Fig. 7 The phylogenetic trees constructed based on *M. figo* and other 14 plant mitogenomes and plastomes. The bootstrap values are clearly displayed within each node. The utilization of distinct colors serves to show the various groups to which the specific species belong. (a) The tree was constructed based on 18 shared mitochondrial genes. (b) The tree was constructed based on 61 shared plastid genes.

Conclusions

In this study, we have successfully sequenced and assembled the mitogenome of *M. figo* for the first time. The circular mitogenome of *M. figo* is 773,377 bp in length, encoding 41 PCGs, 21 tRNA genes and three rRNA genes. A total of 22 *cis*- and three *trans*-splicing introns were identified in the *M. figo* mitogenome. The *M. figo* mitogenome contains abundant repeats, with 1,514 pairs of dispersed repeats, 39 tandem repeats, and 262 SSRs. Additionally, we identified 81 fragments (42,791 bp) that were transferred from the plastome to the mitogenome of *M. figo*, constituting 5.53% of the whole mitogenome. The *M. figo* mitogenome is characterized by the abundance of repeats and MTPTs, contributing to the complexity and diversity of mitogenome size and structure. Furthermore, comparative analyses of four Magnoliaceae mitogenomes reveal significant genetic diversity of this genus. Two phylogenetic trees, constructed independently based on the mitogenomes and plastomes of 15 species, depicted the phylogenetic relationship of *M. figo*. This study presents the first comprehensive genomic and phylogenetic analyses of the *M. figo* mitogenome, providing crucial theoretical insights and data support for the development of genetic markers, classification, and resource utilization within the *Michelia* genus.

Ethical statements

This study has rigorously adhered to relevant institutional, national, and international guidelines and regulations. Moreover, the study did not involve the use of any endangered or protected species. The *M. figo* plant leaves utilized in this experiment were collected at Nanjing Forestry University.

Author contributions

The authors confirm contribution to the paper as follows: study conception and design: Bi C, Yang Y; analysis and interpretation of results: Wang S, Sun N, Qiu J, Han F; materials collection and experiments conduct: Bi C, Qiu J; draft manuscript preparation:Wang S; manuscript revision presentation of comments: Bi C, Wang Z, Yang Y. All authors reviewed the results and approved the final version of the manuscript.

Data availability

The mitochondrial genome supporting this study is available at GenBank with accession number: NC_082234.1. The HiFi sequencing data of *M. figo* is deposited in the SRA repository under SRR28267342.

Acknowledgments

The work is supported by the Natural Science Foundation of Jiangsu Province (BK20220414) and Jiangsu Students' Innovation and Entrepreneurship Training Program (202210298119Y). We thank Assoc. Prof. Kewang Xu from Nanjing Forestry University for collecting the sample of *M. figo*.

Conflict of interest

The authors declare that they have no conflict of interest.

Supplementary information accompanies this paper at (https://www.maxapress.com/article/doi/10.48130/gcomm-0025-0001)

Dates

Received 24 November 2024; Revised 3 January 2025; Accepted 7 January 2025; Published online 24 January 2025

References

1. Roger AJ, Muñoz-Gómez SA, Kamikawa R. 2017. The origin and diversification of mitochondria. *Current Biology* 27(21):R1177–R1192
2. Dyall SD, Brown MT, Johnson PJ. 2004. Ancient invasions: from endosymbionts to organelles. *Science* 304:253–57
3. Yu SB, Pekkurnaz G. 2018. Mechanisms orchestrating mitochondrial dynamics for energy homeostasis. *Journal of Molecular Biology* 430:3922–41
4. van Loo G, Saelens X, van Gurp M, MacFarlane M, Martin SJ, et al. 2002. The role of mitochondrial factors in apoptosis: a Russian roulette with more than one bullet. *Cell Death & Differentiation* 9:1031–42
5. Bi C, Sun N, Han F, Xu K, Yang Y, et al. 2024. The first mitogenome of Lauraceae (*Cinnamomum chekiangense*). *Plant Diversity* 46:144–48
6. Ma Q, Wang Y, Li S, Wen J, Zhu L, et al. 2022. Assembly and comparative analysis of the first complete mitochondrial genome of Acer truncatum Bunge: a woody oil-tree species producing nervonic acid. *BMC Plant Biology* 22:29
7. Han F, Qu Y, Chen Y, Xu LA, Bi C. 2022. Assembly and comparative analysis of the complete mitochondrial genome of Salix wilsonii using PacBio HiFi sequencing. *Frontiers in Plant Science* 13:1031769
8. Wang XD, Xu CY, Zheng YJ, Wu YF, Zhang YT, et al. 2022. Chromosome-level genome assembly and resequencing of camphor tree (*Cinnamomum camphora*) provides insight into phylogeny and diversification of terpenoid and triglyceride biosynthesis of Cinnamomum. *Horticulture Research* 9:uhac216
9. Morley SA, Nielsen BL. 2017. Plant mitochondrial DNA. *Frontiers in Bioscience-Landmark (FBL)* 22:1023–32
10. Wynn EL, Christensen AC. 2019. Repeats of unusual size in plant mitochondrial genomes: identification, incidence and evolution. *G3 Genes| Genomes| Genetics* 9:549–59
11. Møller IM, Rasmusson AG, Van Aken O. 2021. Plant mitochondria – past, present and future. *The Plant Journal* 108:912–59
12. Skippington E, Barkman TJ, Rice DW, Palmer JD. 2015. Miniaturized mitogenome of the parasitic plant *Viscum scurruloideum* is extremely divergent and dynamic and has lost all nad genes. *Proceedings of the National Academy of Sciences of the United States of America* 112:E3515–E24
13. Putintseva YA, Bondar EI, Simonov EP, Sharov VV, Oreshkova NV, et al. 2020. *Siberian larch* (*Larix sibirica* Ledeb.) mitochondrial genome assembled using both short and long nucleotide sequence reads is currently the largest known mitogenome. *BMC Genomics* 21:654
14. Bi C, Qu Y, Hou J, Wu K, Ye N, et al. 2022. Deciphering the Multi-Chromosomal Mitochondrial Genome of *Populus simonii*. *Frontiers in Plant Science* 13:914635
15. Logacheva MD, Schelkunov MI, Fesenko AN, Kasianov AS, Penin AA. 2020. Mitochondrial genome of *Fagopyrum esculentum* and the genetic diversity of extranuclear genomes in buckwheat. *Plants* 9:618
16. Adams KL, Qiu YL, Stoutemyer M, Palmer JD. 2002. Punctuated evolution of mitochondrial gene content: High and variable rates of mitochondrial gene loss and transfer to the nucleus during angiosperm evolution. *Proceedings of the National Academy of Sciences of the United States of America* 99:9905–12
17. Filip E, Skuza L. 2021. Horizontal gene transfer involving chloroplasts. *International Journal of Molecular Sciences* 22:4484
18. Rodríguez-Moreno L, González VM, Benjak A, Carmen Martí M, Puigdomènech P, et al. 2011. Determination of the melon chloroplast and mitochondrial genome sequences reveals that the largest reported mitochondrial genome in plants contains a significant amount of DNA having a nuclear origin. *BMC Genomics* 12:424
19. Veltjen E, Testé E, Palmarola Bejerano A, et al. 2022. The evolutionary history of the Caribbean magnolias (Magnoliaceae): Testing species delimitations and biogeographical hypotheses using molecular data. *Molecular Phylogenetics and Evolution* 167:107359
20. Law YW. 1984. A preliminary study on the taxonomy of the family magnoliaceae. *Journal of Systematics and Evolution* 22(2):89–109
21. Taprial S. 2015. A review on phytochemical and pharmacological properties of *Michelia champaca* Linn. family: Magnoliaceae. *International Journal Of Pharmaceutical Sciences And Research* 2:430–36
22. Shang C, Hu Y, Deng C, Hu K. 2002. Rapid determination of volatile constituents of *Michelia alba* flowers by gas chromatography-mass spectrometry with solid-phase microextraction. *Journal of chromatography. A* 942:283–8
23. Khan MR, Kihara M, Omoloso AD. 2002. Antimicrobial activity of *Michelia champaca*. *Fitoterapia* 73:744–48
24. Cheng KK, Nadri MH, Othman NZ, Rashid SNAA, Lim YC, et al. 2022. Phytochemistry, bioactivities and traditional uses of *Michelia* × *alba*. *Molecules* 27:3450
25. Chericoni S, Testai L, Campeol E, Calderone V, Morelli I, et al. 2004. Vasodilator activity of *Michelia figo Spreng* (Magnoliaceae) by in vitro functional study. *Journal of Ethnopharmacology* 91:263–66
26. Zhai M. 2020. The complete chloroplast genome sequence of *Michelia figo* based on landscape design, and a comparative analysis with other *Michelia* species. *Mitochondrial DNA Part B* 5:2723–24
27. Hinsinger DD, Strijk JS. 2017. The chloroplast genome sequence of *Michelia alba* (Magnoliaceae), an ornamental tree species. *Mitochondrial DNA Part B* 2:9–10
28. Li Y, Zhou M, Wang L, Wang J. 2021. The characteristics of the chloroplast genome of the *Michelia chartacea* (Magnoliaceae). *Mitochondrial DNA Part B* 6:493–95
29. Sima Y, Li Y, Yuan X, Wang Y. 2020. The complete chloroplast genome sequence of *Michelia chapensis* Dandy: an endangered species in China. *Mitochondrial DNA Part B* 5:1594–95
30. Arseneau JR, Steeves R, Laflamme M. 2017. Modified low-salt CTAB extraction of high-quality DNA from contaminant-rich tissues. *Molecular Ecology Resources* 17:686–93
31. Shi Q, Tian D, Wang J, Chen A, Miao Y, et al. 2023. Overexpression of miR390b promotes stem elongation and height growth in *Populus*. *Horticulture Research* 10:uhac258
32. Bi C, Shen F, Han F, Qu Y, Hou J, et al. 2024. PMAT: an efficient plant mitogenome assembly toolkit using low coverage HiFi sequencing data. *Horticulture Research* 11:uhae023
33. Dong S, Chen L, Liu Y, Wang Y, Zhang S, et al. 2020. The draft mitochondrial genome of Magnolia biondii and mitochondrial phylogenomics of angiosperms. *Plos One* 15:e0231020
34. Wick RR, Schultz MB, Zobel J, Holt KE. 2015. Bandage: interactive visualization of de novo genome assemblies. *Bioinformatics* 31:3350–52
35. Li J, Ni Y, Lu Q, Chen H, Liu C. 2024. PMGA: A plant mitochondrial genome annotator. *Plant Communications* 00:101191
36. Chen Y, Ye W, Zhang Y, Xu Y. 2015. High speed BLASTN: an accelerated MegaBLAST search tool. *Nucleic Acids Research* 43:7762–68
37. Lowe TM, Eddy SR. 1997. tRNAscan-SE: a program for improved detection of transfer RNA genes in genomic sequence. *Nucleic Acids Research* 25:955–64
38. Zhang X, Chen H, Ni Y, Wu B, Li J, et al. 2024. Plant mitochondrial genome map (PMGmap): a software tool for the comprehensive visualization of coding, noncoding and genome features of plant mitochondrial genomes. *Molecular Ecology Resources* 24:e13952

39. Beier S, Thiel T, Münch T, Scholz U, Mascher M. 2017. MISA-web: a web server for microsatellite prediction. *Bioinformatics* 33:2583–85
40. Benson G. 1999. Tandem repeats finder: a program to analyze DNA sequences. *Nucleic Acids Research* 27:573–80
41. Kurtz S, Choudhuri JV, Ohlebusch E, Schleiermacher C, Stoye J, et a l. 2001. REPuter: the manifold applications of repeat analysis on a genomic scale. *Nucleic Acids Research* 29:4633–42
42. Mao J, Wei S, Chen Y, Yang Y, Yin T. 2023. The proposed role of MSL-lncRNAs in causing sex lability of female poplars. *Horticulture Research* 10:uhad042
43. Chen C, Wu Y, Li J, Wang X, Zeng Z, et al. 2023. TBtools-II: a "one for all, all for one" bioinformatics platform for biological big-data mining. *Molecular Plant* 16:1733–42
44. Marçais G, Delcher AL, Phillippy AM, Coston R, Salzberg SL, et al. 2018. MUMmer4: A fast and versatile genome alignment system. *PLOS Computational Biology* 14:e1005944
45. He W, Yang J, Jing Y, Xu L, Yu K, et al. 2023. NGenomeSyn: an easy-to-use and flexible tool for publication-ready visualization of syntenic relationships across multiple genomes. *Bioinformatics* 39:btad121
46. Katoh K, Rozewicki J, Yamada KD. 2019. MAFFT online service: multiple sequence alignment, interactive sequence choice and visualization. *Briefings in Bioinformatics* 20:1160–66
47. Capella-Gutiérrez S, Silla-Martínez JM, Gabaldón T. 2009. trimAl: a tool for automated alignment trimming in large-scale phylogenetic analyses. *Bioinformatics* 25:1972–73
48. Nguyen LT, Schmidt HA, von Haeseler A, Minh BQ. 2015. IQ-TREE: a fast and effective stochastic algorithm for estimating maximum-likelihood phylogenies. *Molecular Biology and Evolution* 32:268–74
49. Stamatakis A. 2006. RAxML-VI-HPC: maximum likelihood-based phylogenetic analyses with thousands of taxa and mixed models. *Bioinformatics* 22:2688–90
50. Letunic I, Bork P. 2021. Interactive tree of life (iTOL) v5: an online tool for phylogenetic tree display and annotation. *Nucleic Acids Research* 49:W293–W296
51. Wu ZQ, Liao XZ, Zhang XN, Tembrock LR, Broz A. 2022. Genomic architectural variation of plant mitochondria—A review of multichromosomal structuring. *Journal of Systematics and Evolution* 60:160–68
52. Sloan DB, Alverson AJ, Chuckalovcak JP, Wu M, McCauley DE, et al. 2012. Rapid evolution of enormous, multichromosomal genomes in flowering plant mitochondria with exceptionally high mutation rates. *PLoS Biology* 10:e1001241
53. Alverson AJ, Wei X, Rice DW, Stern DB, Barry K, et al. 2010. Insights into the evolution of mitochondrial genome size from complete sequences of *Citrullus lanatus* and *Cucurbita pepo* (Cucurbitaceae). *Molecular Biology and Evolution* 27:1436–48
54. Gualberto JM, Newton KJ. 2017. Plant mitochondrial genomes: dynamics and mechanisms of mutation. *Annual Review of Plant Biology* 68:225–52
55. Gualberto JM, Mileshina D, Wallet C, Niazi AK, Weber-Lotfi F, et al. 2014. The plant mitochondrial genome: dynamics and maintenance. *Biochimie* 100:107–20
56. Rice DW, Alverson AJ, Richardson AO, Young GJ, Sanchez-Puerta MV, et al. 2013. Horizontal transfer of entire genomes via mitochondrial fusion in the angiosperm *Amborella*. *Science* 342:1468–73
57. Yu R, Sun C, Zhong Y, Liu Y, Sanchez-Puerta MV, et al. 2022. The minicircular and extremely heteroplasmic mitogenome of the holoparasitic plant *Rhopalocnemis phalloides*. *Current Biology* 32:470–479.e5
58. Yang H, Ni Y, Zhang X, Li J, Chen H, et al. 2023. The mitochondrial genomes of *Panax notoginseng* reveal recombination mediated by repeats associated with DNA replication. *International Journal of Biological Macromolecules* 252:126359
59. Cole LW, Guo W, Mower JP, Palmer JD. 2018. High and variable rates of repeat-mediated mitochondrial genome rearrangement in a genus of plants. *Molecular Biology and Evolution* 35:2773–85
60. Sun M, Zhang M, Chen X, Liu Y, Liu B, et al. 2022. Rearrangement and domestication as drivers of Rosaceae mitogenome plasticity. *BMC Biology* 20:181
61. Zardoya R. 2020. Recent advances in understanding mitochondrial genome diversity. *F1000Research* 9:270
62. Richardson AO, Rice DW, Young GJ, Alverson AJ, Palmer JD. 2013. The "fossilized" mitochondrial genome of *Liriodendron tulipifera*: ancestral gene content and order, ancestral editing sites, and extraordinarily low mutation rate. *BMC Biology* 11:29
63. Mower JP, Sloan DB, Alverson AJ. 2012. Plant mitochondrial genome diversity: The genomics revolution. In *Plant Genome Diversity Volume 1: Plant Genomes, their Residents, and their Evolutionary Dynamics*, ed. JF Wendel, J Greilhuber, J Dolezel, IJ Leitch: 123-44. Vienna: Springer Vienna. Number of 123-44 pp
64. Sloan DB, Alverson AJ, Štorchová H, Palmer JD, Taylor DR. 2010. Extensive loss of translational genes in the structurally dynamic mitochondrial genome of the angiosperm *Silene latifolia*. *BMC Evolutionary Biology* 10:274
65. Hecht J, Grewe F, Knoop V. 2011. Extreme RNA editing in coding islands and abundant microsatellites in repeat sequences of *Selaginella moellendorffii* mitochondria: the root of frequent plant mtDNA recombination in early tracheophytes. *Genome Biology and Evolution* 3:344–58
66. Regina TMR, Quagliariello C. 2010. Lineage-specific group II intron gains and losses of the mitochondrial *rps3* gene in gymnosperms. *Plant Physiology and Biochemistry* 48:646–54
67. Timmis JN, Ayliffe MA, Huang CY, Martin W. 2004. Endosymbiotic gene transfer: organelle genomes forge eukaryotic chromosomes. *Nature Reviews Genetics* 5:123–35
68. Cheng Y, He X, Priyadarshani SVGN, Wang Y, Ye L, et al. 2021. Assembly and comparative analysis of the complete mitochondrial genome of *Suaeda glauca*. *BMC Genomics* 22:167
69. Sloan DB, Wu Z. 2014. History of plastid DNA insertions reveals weak deletion and AT mutation biases in angiosperm mitochondrial genomes. *Genome Biology and Evolution* 6:3210–21
70. Zhang T, Fang Y, Wang X, Deng X, Zhang X, et al. 2012. The complete chloroplast and mitochondrial genome sequences of *Boea hygrometrica*: insights into the evolution of plant organellar genomes. *PLOS ONE* 7:e30531
71. Wang D, Rousseau-Gueutin M, Timmis JN. 2012. Plastid sequences contribute to some plant mitochondrial genes. *Molecular Biology and Evolution* 29:1707–11
72. Wang D, Wu YW, Shih AC, Wu CS, Wang YN, et al. 2007. Transfer of Chloroplast Genomic DNA to Mitochondrial Genome Occurred At Least 300 MYA. *Molecular Biology and Evolution* 24:2040–48
73. Notsu Y, Masood S, Nishikawa T, Kubo N, Akiduki G, et al. 2002. The complete sequence of the rice (*Oryza sativa* L.) mitochondrial genome: frequent DNA sequence acquisition and loss during the evolution of flowering plants. *Molecular Genetics and Genomics* 268:434–45
74. Clifton SW, Minx P, Fauron CMR, Gibson M, Allen JO, et al. 2004. Sequence and Comparative Analysis of the Maize NB Mitochondrial Genome. *Plant Physiology* 136:3486–503
75. Nie ZL, Wen J, Azuma H, Qiu YL, Sun H, et al. 2008. Phylogenetic and biogeographic complexity of Magnoliaceae in the Northern Hemisphere inferred from three nuclear data sets. *Molecular Phylogenetics and Evolution* 48:1027–40
76. Group TAP, Chase MW, Christenhusz MJM, Fay MF, Byng JW, et al. 2016. An update of the Angiosperm Phylogeny Group classification for the orders and families of flowering plants: APG IV. *Botanical Journal of the Linnean Society* 181:1–20